Bayesian Networks and CFD Model of a Chemical Vapor Deposition to Design a Carbon Nanotubes Reactor

Karla Adriana Morales Vázquez[1], Irving César Ortiz Vázquez[1], Rodrigo Fernandez-Loyola[1], Miriam Rocío Estevez González[3], Juan Francisco Pérez Robles[1], *Guillermo Alfonso De la Torre Gea[2].

1. CINVESTAV Instituto Politécnico Nacional, Libramiento Nor-Poniente No. 2000, Real de Juriquilla, C.P. 76230, Queretaro, Qro.
2. Instituto de Investigación y Desarrollo de Tecnologías GARMAN, Av. Andamaxei 64-40, Corregidora, Qro., Mexico. C.P. 76910.
3. Centro de Física Aplicada y Tecnología Avanzada, (CFATA), Universidad Nacional Autónoma de México (UNAM) , , Boulevard Juriquilla # 3001 Juriquilla, Queretaro, Qro., Mexico. C.P. 76230.

*Corresponding author: (+52) 4421260280, gtorre@abanet.mx

***Abstract*—The use of chemical vapor deposition technique has increased in the last five years, mainly due to the thin film production, such as graphene sheets for photovoltaic applications, carbon nanotubes films as catalysts, and semiconductors films as electrodes in electronic devices. If turbulence is increased in those processes, also mixing of solution and growth rate of nanotubes are increased. Then, the incidence angle of doping species influences the laminar flow of reaction gas, and therefore, the amount of carbon nanotubes obtained in the quantification. Many studies choose Computational Fluid Dynamics (CFD) models to obtain the best operating conditions for physical systems and design evaluations. Thus, we developed a Computational Fluid Dynamics model of a Chemical Vapor Deposition type reactor, where flows were simulated for different species of gases, to assess the ideal conditions to improve the production process of carbon nanotubes. We used Bayesian Network probability model and determined the inference of eddy turbulence over the flow yield. We found that flow systems increase directly production and metal attachment to the nanotubes network with an insertion at 90°, because gas presence in the reaction zone is favored. The model allows us to quantify the eddy viscosity and its probability along the reactor to improve further designs.**

***Keywords*—Bayesian networks, CFD, carbon nanotubes, CVD, eddy viscosity.**

I. INTRODUCTION

Chemical Vapor Deposition (CVD) is a versatile process in which the gas phase molecules decompose the reactive species for particle growth. In this method, a substrate that acts as a catalyst (Fe, Co, Ni) produces a thin film of 1 to 50 nm thick, which is heated in a furnace with inert helium at a low pressure. When temperature reaches 600 ° C, with the slow addition of methane, acetylene, or benzene, carbon atoms are released and could recombine as nanotubes [3].

The metal is bonded separately due to the high temperatures in CVD process; those nanoparticles serve as growth centers, forming the basis of nanotubes. Therefore, the particle size defines the diameter of the nanotube obtained [7,14,11]. The CVD process could be simulated with the aim to find the best condition to obtain the nanoparticles. Using a Computational Fluid Dynamics (CFD) model, Kim *et al*. [12] proved that the structural formation of carbon nanotubes vertically (CNT) in forest array, is primarily affected by the gas flow that leads to direction changes in growth during the CVD process [13].

Many studies have been conducted using CFD model to determine the best operational conditions of these systems. In consequence, it has increased systems performance, and predicted their results. Choi *et al*. [4] developed a multiscale computational framework, with a couple of continuum model simulations and molecular dynamics method for manufacturing nanotubes materials, in which validation was performed for the plasma - assisted growth. Ismail *et*

al. [10] investigated thermal conditions of the fluid aligned and staggered multi-walled CNT (MWCNT) using a numerical method based on micro pin fins having 650 microns long hydraulic diameter of 130 microns. Heat transfer coefficients were obtained for effective heat fluxes ranging from 50 to 130 W and Reynolds numbers 14-160.

A research review was reported by Raji and Sobhan [17] about the simulation of nucleation processes and growth of carbon nanotubes, using different modeling techniques. Modeling methods include CFD conventional approaches and techniques of discrete computer. Nano fluidic technology is advancing rapidly and with it, series of new technical opportunities are emerging. However, the prediction rate and heat transfer in the low mass of nano-scale systems presents a major obstacle to its design. The existence of no continuing effects, such as molecular stratification and sliding speed near the liquid-solid interfaces, apparently excludes continuous efficient CFD [9].

Van Santen *et al.* [20] determined, with a 2D CFD model, that the turbulence increase mixing and growth rate of nanotubes, then the incidence angle of doping species influences the laminar flow of reaction gas, and therefore, the amount of carbon nanotubes obtained in the quantification. Although numerous studies had been conducted with reactors using CFD as a tool to calculate realistic approaches, nevertheless, there is not yet an optimal design for a CVD type reactor. The objective of this study is to develop an efficient CVD reactor design for the production of carbon nanotubes using a CFD model changing the entries of fluids in 90° from the outlet direction.

II. CFD THEORY

CFD method is based on the fluid dynamics equations (continuity, momentum, and energy). The equations obtained directly from the volume or fixed element in space are known as "conservative form". While the equations obtained from the volume and move with the fluid element are called "non-conservative form".

The substantial derivative is physically the exchange rate of any substance that moves with a fluid element. It consists of two parts; the first part is called the local derivative, which is physically the rate of change overtime in a fixed point. The second part is called the convective derivative, which is physically the exchange rate due to movement of the fluid from one point to another in the field of fluid, where the fluid properties are spatially different. The resulting material can be applied to any field variable fluid, for example: pressure (p) or temperature (T) [1].

$$\nabla \equiv i\frac{\partial}{\partial x} + j\frac{\partial}{\partial y} + k\frac{\partial}{\partial z}$$

$$V \equiv (u, v, w) \qquad \textbf{(1)}$$

$$\frac{\partial}{\partial t}\iiint_V \rho dV + \iint_S \rho V \cdot dS = 0 \qquad \textbf{(2)}$$

$$\rho\frac{Du}{Dt} = -\frac{\partial p}{\partial x} + \frac{\partial t_{xx}}{\partial x} + \frac{\partial t_{yx}}{\partial x} + \frac{\partial t_{zx}}{\partial x} + \rho f_x$$

$$\rho\frac{Dv}{Dt} = -\frac{\partial p}{\partial x} + \frac{\partial t_{xy}}{\partial x} + \frac{\partial t_{yy}}{\partial x} + \frac{\partial t_{zy}}{\partial x} + \rho f_y$$

$$\rho\frac{Dw}{Dt} = -\frac{\partial p}{\partial x} + \frac{\partial t_{xz}}{\partial x} + \frac{\partial t_{yz}}{\partial x} + \frac{\partial t_{zz}}{\partial x} + \rho f_z \qquad \textbf{(3)}$$

$$\rho\frac{Dw}{Dt}\left(e+\frac{V^2}{2}\right) = \rho q + \frac{\partial}{\partial x}\left(k+\frac{\partial T}{\partial x}\right) + \frac{\partial}{\partial y}\left(k+\frac{\partial T}{\partial y}\right) + \frac{\partial}{\partial z}\left(k+\frac{\partial T}{\partial z}\right) - \frac{\partial(up)}{\partial x} - \frac{\partial(vp)}{\partial y} - \frac{\partial(wp)}{\partial z}$$
$$+ \frac{\partial(ut_{xx})}{\partial x} + \frac{\partial(ut_{yx})}{\partial y} + \frac{\partial(ut_{zx})}{\partial z} + \frac{\partial(vt_{xy})}{\partial x} + \frac{\partial(vt_{yy})}{\partial y} + \frac{\partial(vt_{zy})}{\partial z}$$
$$+ \frac{\partial(wt_{xz})}{\partial x} + \frac{\partial(wt_{yz})}{\partial y} + \frac{\partial(wt_{zz})}{\partial z} + pf \cdot V \qquad \textbf{(4)}$$

Where,

1) Continuity Equation

2) Momentum Equation (a non-conservative)

3) Components in x, y and z

4) Energy Equation (a non-conservative)

The equations form a coupled system of partial differential nonlinear equations. So far, no analytical solution has been found. It is commonly assumed that the fluid is an ideal gas where the intermolecular forces can be neglected. For an ideal gas equation of state:

$$p = \rho RT \quad (5)$$

Where, R is the specific gas constant. For a calorically ideal gas, we have:

$$e = CvT \quad (6)$$

Where, Cv is the specific heat at constant volume [5].

III. Materials and Methods

The work was done in CINVESTAV - Queretaro, using a CVD reactor. The reaction tube is made of stainless steel - AISI 310 schedules 10, with an external diameter of 21.2 cm and length of 1.8 m, as shown in Figure 1.

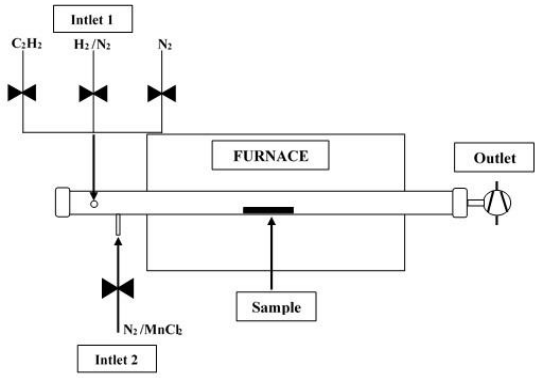

Figure 1. CVD – Reactor.

3.1 Experimental measurements

According with the theoretical work mentioned above, we conducted three different experiments in order to show how the MWCNTs growth in the CVD reactor with the same conditions. 300 milligram of catalyst mixture powder (FeCo) was dispersed inside a small 316 stainless steel container (4 x 2.5 cm) and this container was placed inside the iron tube of the CVD reactor. The stainless steel container were place approximately at 25 cm from the top of the tube for the first experiment, 60 cm from the top of the tube for the second experiment and 97 cm from the top of the tube for the third experiment as show in the next Figure 2.

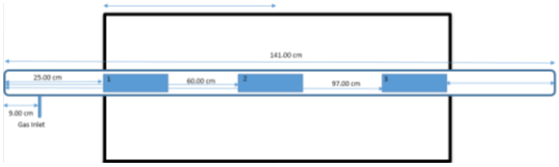

Figure 2.Schematic distribution of the position of the stainless steel container for MWCNTs synthesis.

3.2 CFD Model

The model was developed by CFD ANSYS FLUENT 14.0 software; the simulation was performed according to previous references [5,16,21,24]. First, the dimensional geometry is generated and later proceeds to a tetrahedral meshing type with a characteristic meshing angle of 30° and 20 nodes, as shown in Figure 3. Subsequently, the initial and boundary values shown in Table 1 were obtained from the standards noted patent.

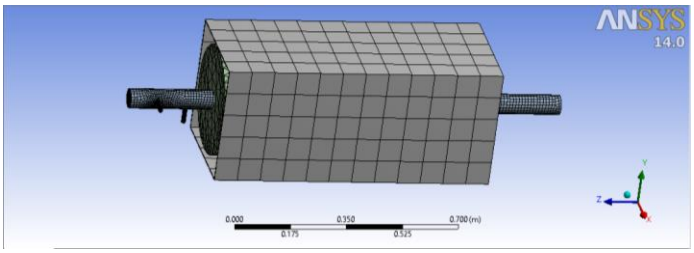

Figure 3.CVD – Reactor meshing.

Table 1. CFD Model configuration

	DESCRIPTION	VALUE		
Solver	3D Simulation			
Condition time	Transcendent			
Viscosity model	k-epsilon (2 eq.), realizable, viscous heating			
Energy equation	Active			
Species	Species transport: Nitrogen, Hydrogen and Acetylene			
Dominion entrance	Velocity intlet 1	0.00014 m/s		
	Pressure intlet 1	275790 Pa		
	Velocity intlet 2	0.00024 m/s		
	Pressure intlet 2	275790 Pa		
Dominion exit	Pressure outlet	-53328.0 Pa		
	Temperature outlet	917.15 K		
Temperature	300 K			
Physical mixtures				
Properties	Nitrogen	Hydrogen	Acetylene	
Enthalpy J/Glom	0.0	0.0	227.48	
Entropy J/Glom	191.5	130.7	200.9	
Temperature K	298.15	298.15	298.15	
Energy	100			

The physical-thermal characterization were consisted in a temperature sampling in 86 points distributed homogeneously of the CVD reactor, in which 14 points were found in the reaction tube, and 72 points in the heating body. The measurement was made by temperature and speeds flow sensors.

The results of solving equations corresponded to the value of the field variables at each grid point. This amount of numbers should be reduced to the basics to be handled with ease and get significant results in the calculation. An important part of this step is the graphical representation of the variables that govern the flow, to have a quick view of the results obtained. Here is also included the comparison of results obtained:

a) Using CFD analysis.
b) With other experimental results.
c) With results from other scientific publications.
d) Against results obtained with Bayesian networks.

3.3 Bayesian Network analysis method

Expected probability distribution of output variables (eq. 7) is determined by the algorithm of solution of the BN. This technique has been used to identify relationships between seemingly indeterminate variables, describing, and quantifying these relationships even with a set of missing data [8,19, 22].

$$P(x_1,\ldots,x_n) = \prod_{i=1}^{n} P(x_i \mid parents\ (x_i)) \quad (7)$$

The result of this calculation (eq. 8) depends on the probability distribution of the input variables. BN is a joint probabilities distribution of a collection of discrete random variables [6,23,24].

$$P(cj \mid xi) = P(xi \mid cj\ )\ P(cj\ )\ /\ k\ P(xi \mid ck\ )\ P(ck\ ) \quad (8)$$

The aim of BN structure learning is to find a configuration that best describes the observed data. Statistical machine learning methods had been applied in the Bayesian statistics; however, machine learning could employ a variety of classification techniques to produce models other than BN. The number of possible structures of direct acyclic graph for searching is exponential in the number of variables in the domain (eq.3). Machine learning could be seen as an attempt to automate some parts of the scientific method by mathematical methods [2].

$$f\ (n) \sum_{i=1}^{n} = (-1)\ I\ +1C_{in}\ 2_i(n\text{-}i)\ f(n\text{-}i\ ) \quad (9)$$

The supervised learning algorithm produces a function that establishes a correspondence between inputs and desired outputs of the system using a node class. On the other hand, all the modeling process is carried out on a set of examples formed just by logging into the system in the unsupervised learning. The simple Bayesian classifier (Naive Bayes classifier, NBC) assumes that attributes are independent of each other given the class and the probability. Each attribute given the class node could be obtained by the product of individual conditional probabilities..

When the model has a structure determinate and the user have complete and sufficient data for all variables, is relatively easy to obtain parameters. The most common method is called maximum likelihood estimator under which the probabilities based on the frequency data are estimated.

- IV RESULTS AND DISCUSSION

According to laboratory work, the first observation during the experiment showed a significant change in the growth of carbon nanotubes depending on the position in which the containers are located. This change is directly reflected in the percentage of production of carbon nanotubes due to the flow of precursor gases. The container located in position (1) produced 157% of MWCNTs, container located in position (2) produce 180% of MWCNTs which means the reaction time of the precursor gas in this part of the reactor is considerable more efficient due to the turbulent flow achieved. The position (3) produce 32% of MWCNTs less than the others experiments, this could be related to the vacuum pump which produce a laminar flow and the reaction time in this position is less than the other positions .

In addition, it was found that flow systems directly increased the nanotubes production, and the amount of metal attached to the network of the nanotubes, resulting in a greater measure and equal quality insertion at 180° observed flow in the system, and at 90 °, the gas residence in the reaction zone was favored.

CFD simulation models exhibit greater temperature rise when the gas flow was introduced at 90°, indicating that the process is more efficient. Other simulation model reported by references [15,18], a dynamic CFD model over time to determine the fluid flow in the first few seconds was performed in the present work, as shown in Figure 4.

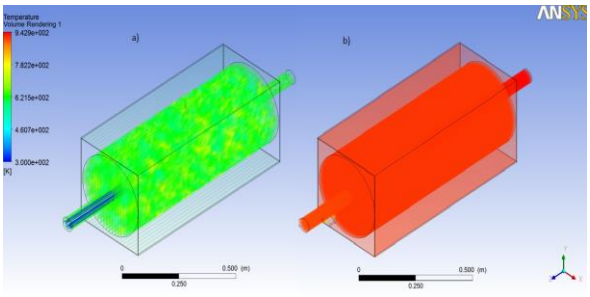

Figure 4. Temperature in a CVD – Reactor: a) at 180° and b) at 90°.

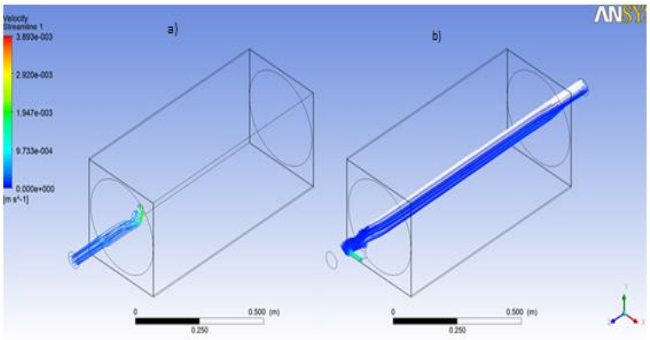

Figure 5. Fluid flow in a CVD – Reactor: a) at 180° and b) at 90°.

After 30 seconds into the CVD process, the fluid traveled almost the entire reactor when it was added at 90°, moreover, it was observed that by adding it to 180° the fluid does not reach into the reaction zone, because it has a laminar flow (Fig. 5).

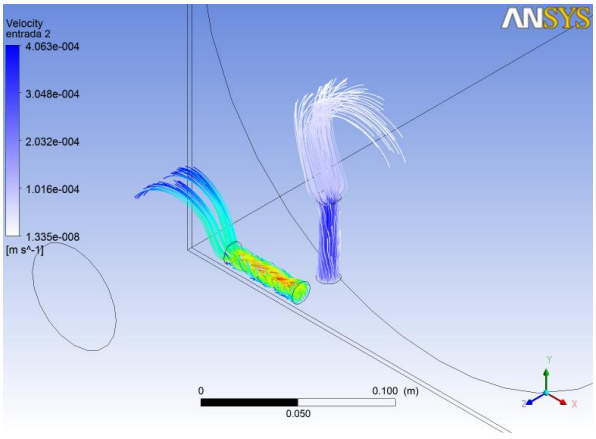

Figure 6. Fuid flow inlet CVD – Reactor at 90°.

Figure 6 showed fluid inlet in the process, where we appreciate the direction of flow turbulently. A turbulent flow has characteristics in many different length scales, all of which interact. In this model, additional turbulence tensions occur by increasing the molecular viscosity, with an eddy viscosity (Figure 6). This information allowed to quantify the eddy viscosity along the reactor for subsequent designs.

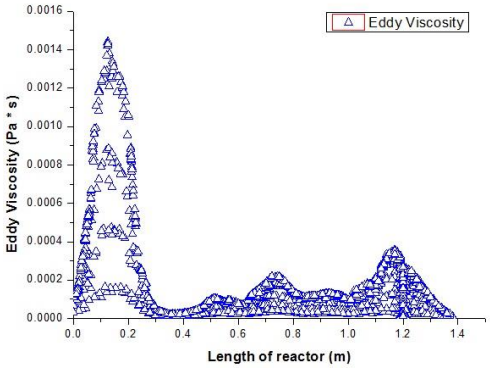

Figure 6. Fuid flow inlet CVD – Reactor at 90°.

This effect could be seen primarily by the bulk amount of carbon nanotubes obtained in the system, based on 0.5 g of FeCo. We proceeded to make the bulk amount of nanotubes, obtained on completion of the reaction and the amount after purification process, and the atomic percentage of manganese in the samples obtained by Energy Dispersive Spectroscopy analysis (EDS), how is showed in Table 2:

Table 2.Comparative performance – fluid flow.

Inlet flow	MWNT´S-Mn without purify (gr)	MWNT´S-Mn purify (gr)	Atomic percent (%)
180°	1.345	0.824	0.87 ± 0.05
90°	1.875	1.002	1.25 ± 0.05

The classic model of naïve Bayes was built with all predictor variables, i.e., it was assumed that these variables are independent of the class. With these results, an analysis was conducted using the software Elvira to determine the BN model structure. This process was marked as non-supervised classification method.

Figure 7 shows the result of unsupervised clustering or classification, where the class node establishes a bridge between the variables relating them is according to Bayes' theorem. The variable z, which corresponds to the length of the reactor, was the only replay showing a direct relationship with the node class. Moreover, the variable y, which corresponds to the height of the reactor, was inversely proportional to the node class. The turbulence (eddy) had an indeterminate relationship.

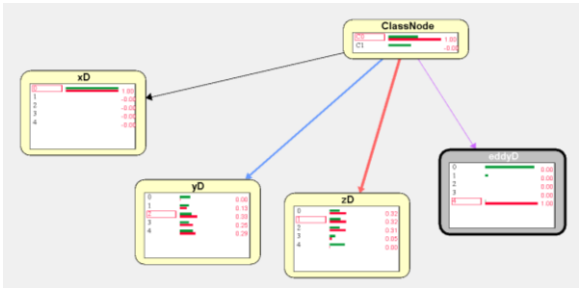

Figure 7.Supervised classifier.

According to Bayesian analysis, the greater turbulence was equal to 0.00145 Pa*s and was presented between 0 - 0.768 m length with 0.95% of conditional probability, and between -0.06 - 0.01 m the length axis, with 0.87% of conditional probability.

V. Conclusions

From analysis using CFD, we could understand the physical effect caused by the change in the angle of entry of the reaction gases and obtaining data speed misting system. These data allow us to realize that the residence time of the dopant gas should be higher. This system is ratified by making a comparison with the product output between the two angles, where we were noted that the angle of 90 ° provides greater amount of manganese in the walls of the multiwall carbon nanotube, that widely favors the catalytic function to carry out the process for obtaining synthetic diesel; because with larger amount of catalytic metal available the reaction is favored. The maximum turbulence (equal to 0.00145 Pa*s) was presented between 0 – 0.768 m with 0.95 % of conditional probability. Bayesian Network method allowed us to determine relationships between variables considered independent with classic statistical methods and calculate their inferences.

6. Acknowledgements

This research was partially supported by the Mexican National Council of Science (CONACYT).

Conflicts of Interest
Authors declared no conflicts of interest.

7. References

1. Anderson, J.D. 1995. Computational Fluid Dynamics. McGraw-Hill, US
2. Borunda, M., Jaramillo, O. A., Reyes, A., Ibargüengoytia, P.H. (2016). Bayesian Networks in Renewable Energy Systems: A Bibliographical Survey. Renewable and Sustainable Energy Reviews, 62; 32–45.
3. Che, G., Lakshmi, B. B., Martin, C. R., Fisher, E. R., andRuoff, R. S., 1998. Chemical Vapor Deposition Based Synthesis of Carbon Nanotubes and Nanofibers Using a Template Method. Chemistry of Materials, 10(1), 260–267. doi:10.1021/cm970412f
4. Choi, H. S., Kim, K. H., Hong, K. H., Kim, J., Lee, H. S., Shin, J. K., and Kolobov, V., 2005. Multi-Scale Modeling of Processing of Carbon Nanotubes. NSTI-Nanotech, 2; 1 – 4.
5. De la Torre-Gea, G., Soto-Zarazúa, G. M., López-Crúz, I., Torres-Pacheco, I., and Rico-García, E., 2011. Computational fluid dynamics in greenhouses: A review. African Journal of Biotechnology, 10(77), 17651-17662.
6. Garrote L, Molina M, Mediero L, Probabilistic Forecasts Using Bayesian Networks Calibrated with Deterministic Rainfall- Runoff Models, in Vasilievet al. edited by Extreme Hydrological Events: New Concepts for Security (Springer) 2007, 173.
7. Greendyke, R. B., Stein, T. H., Ray, L. A., Creel, J., Payne, B., & Scott, C. D. (2005). Higher order chemistry models in the CFD simulation of laser-ablated carbon plumes. AIAA Paper, 765.
8. Hruschka E, Hruschka E, Ebecken N F F, Bayesian networks for imputation in classification Problems, J Intell Inform Syst, 29 (2007) 231.
9. Holland, D., Lockerby, D., Borg, M., and Reese, J., 2014. Molecular Dynamics Pre-Simulation Methodology for Nano-Scale Computational Fuid Dynamics. Proceeding 11th.World Congress On Computational Mechanics.
10. Ismail, M., Rashid, M. A. I., and Mahbub, M., 2012. Numerical computation of fluid flow and heat transfer in a MEMS-based micro channel heat sink. Frontiers in Heat and Mass Transfer (FHMT), 3(3).
11. Ji, R. Y., Chan, D. S., Jow, J. J., & Wu, M. S. (2013). Formation of open-ended nickel hydroxide nanotubes on three-dimensional nickel framework for enhanced urea electrolysis. Electrochemistrycommunications, 29, 21-24.
12. Kim, H., Kim, K.S., Kang, J., Park, Y.C., Chun, K.Y., Boo, J.H., Kim, Y.J., Hong, B.H. and Choi, J.B., 2011. Flow-dependent directional growth of carbon nanotube forests by chemical vapor deposition. Nanotechnology 22 095303 (5pp) doi:10.1088/0957-4484/22/9/095303.
13. Kim, K. S., Kingston, C. T., Hrdina, A., Jakubinek, M. B., Guan, J., Plunkett, M. and Simard, B., 2014. Hydrogen-Catalyzed, Pilot-Scale Production of Small Diameter Boron Nitride Nanotubes and Their Macroscopic Assemblies. American Chemical Society, 8(6); 6211 – 6220.
14. Kumar, M., and Ando, Y., 2010. Chemical Vapor Deposition of Carbon Nanotubes: A Review on Growth Mechanism and Mass Production. Journal of Nanoscience and Nanotechnology, 10(6), 3739–3758. doi:10.1166/jnn.2010.2939.
15. Kuwana, K., Andrews, R., Grulke, E. A., and Saito, K., 2001. Synthesis of carbon nanotubes using CVD reactor: numerical simulations of heat and mass transfer, www.adaptive-research.com
16. Ortiz-Vazquez, I. C., Pérez-Robles, J. F., De La Torre-Gea, G. Fernandez-Loyola, R. and Pérez-Brito, J.F., 2015. A Multivariable Computational Fluid Dynamics Analysis Method Based in Bayesian Networks Applied in a Bioreactor. Journal of Applied Chemical Science International; 6(1), 10 – 17.
17. Raji, K., and Sobhan, C. B., 2013. Simulation and modeling of carbon nanotube synthesis: current trends and investigations. Nanotechnology Reviews, 2(1), 73-105.
18. Passos, M. F.,Binelli, A. R. R., Jardini L. A, Dias, C. G. B. T. and Filho, R.M.,2015. CFD Study of Chemical Vapor Deposition Reactor for Synthesis of Phema Chemical Engineering Transactions; 43: 1-6.
19. Reyes P, Bayesian networks for setting genetic algorithm parameters used in problems of geometric constraint satisfaction, Intel. Artificial, 45 (2010) 5.
20. Van Santen, H., Kleijn, C.R. and Van Den Akker, H.E.A., 1998. Large Eddy Simulations in a Rotary Disk Chemical Vapor Deposition

Reactor. PVP-Vol. 377-1, Computational Technologies for Fluid/thermal/Structural/Chemical Systems with Industrial Applications.

21. Ortíz-Vázquez, I.C.; Rodriguez-Mendez, L.I.; Soto-Zarazúa, G., Pérez-Robles, J.F.; Rico-García, E., De La Torre-Gea, G.A. 2016. Analysis of large commercial greenhouses in warm climates using CFD and Bayesian Networks. Journal of Global Ecology and Environment, 5(2); 2454-2644.
22. De la Torre-Gea, G.; Ortiz-Vazquez, I.C.;Rico-Garcia, E.; Guevara-Gonzalez, R.; Morales-Vazquez, K.A.; Rodriguez-Mendez, L.I.; Fernandez-Loyola, R.; Perez-Robles, J.F. (2016). Bayesian Analysis of a CFD Model to the Absorption of Ammonium Concentrations in Zeolite. Journal of Scientific and Engineering Research, 3(4); 258—266.
23. De la Torre-Gea, G.A. and García-Manzo, G. (2016). Multi-sensor Fusion Method Using Bayesian Network for Precise Vehicle Performance Evaluation; 1(4); 146—149.
24. Ortiz-Vazquez, I., Morales-Vazquez, K.A., Rodriguez-Mandez, L.I., Fernandez-Loyola, R.,Perez-Robles, J.F., Soto-Zarazua, G., Rico-García, E., García-Manzo, G., De la Torre-Gea, G.A. (2016). Bayesian Analysis Of A CFD Model To A Wind Turbine Made Of Heliocarpus Wood Bayesian; 3(11); 5849—5852.